

Non-invasive identification of lunar rocks with optical and LiDAR systems M. Gmöhling^{1 5}, S. Köhl^{1 5}, J. Zevering¹, D. Borrmann², S. Ferrari³, L. Penasa⁴, R. Pozzobon⁴, A. Nüchter¹

¹Computer Science XVII – Robotics, Julius-Maximilians-Universität Würzburg, ²Faculty of Electrical Engineering - Technical University of Applied Sciences Würzburg-Schweinfurt, ³Center of Studies and Activities for Space (CISAS) “G. Colombo” - University of Padova, ⁴Department of Geosciences - University of Padova, ⁵These authors contributed equally

Introduction: Exploring lunar lava tubes is a main goal for lunar exploration in the next years. Since their environment is better protected, they potentially contain samples less affected by space weathering. One mission aimed at exploring said tubes is DEADALUS [1], which descends a spherical robot into the lava tubes. DAEDALUS aims to provide multiple solutions for non-invasive material analysis. In this work we focus on generally using compact and non-invasive systems for spectral rock identification with emphasis on H₂O detection.

In order to identify the samples we use two different approaches, one with laser scanners and the other with optical cameras. Both methods utilize multiple devices at different wavelengths. For testing our approaches we select four lunar rock types and use three terrestrial samples of basalt, ilmenite, dunite and anorthosite. In addition, we probe the behavior of these stones with a thin layer of H₂O ice on the surface.

Optical method: The goal is to have a fully automated and non-invasive method for optical identification of lunar rocks. For this purpose we use four identical monochrome cameras from IDS called UI-3160CP-M-GL Rev.2.1 with each a 8mm focal lens and a different wavelength filter. A 3D-printed framework fixates the cameras so that performing the same transformation between the cameras is possible.

The quantum efficiency of the cameras spikes at 600nm wavelength and is below 20% for values lower than 350nm and beyond 850nm. Therefore we select filters at 450nm, 600nm, 700nm and 800nm to cover the whole spectrum. The camera setup has two halogen light sources at the top corners of the framework with the aim of obtaining a uniform brightness on all images.

The cameras need to be calibrated geometrically and radiometrically to avoid constant calibration processes. To compensate different lighting conditions like varying brightness, we use four spectralons with 2%, 50%, 75% and 99% reflectance for radiometric calibration. They

reflect the light equally in the wavelength range from 250nm to 2500nm. For this purpose, we take a photo with all Lambertian targets, detect them via Hough Circle Transform and read out the mean reflectance values. The highest intensity in the image needs to be adjusted just below the maximum value detectable for the cameras in order to maximize the spectrum. We then apply linear regression to the mean intensity values of the spectralons and determine the allowed minimum and maximum values for our brightness spectrum.

We photograph the respective stone together with the spectralons, in order to achieve a higher accuracy regarding the calibration. The detection of the rock sample is currently relying on manually selecting the rock corners in the images and calculating the mean of the intensities inside this area. We normalize this mean with the previously determined minimum and maximum value. A removal of all values outside a 95% sigma band ensures a limitation of outliers. The next step is to compare these adjusted values with a database [2] containing the target values of each rock type for 450nm, 600nm, 700nm and 800nm.

LiDAR method: Subsequently following the wavelengths of the optical systems we use three laser scanners in near-infrared at 865nm, 905nm and 1550nm. The available laser scanners determine these wavelengths.

Using LiDAR subsystems already used for mapping to identify rocks reduces the overall size and weight. DEADALUS already tested the LIVOX MID-100 as the LiDAR subsystem. It operates at 905nm and continuously scans non-repetitive points in a flower shape, with the point cloud becoming denser over time.

The reflectance of water ice has a local minimum at around 1500nm. At this wavelength, a low reflectance value generally indicates H₂O. A RIEGL VZ-400, operating at 1550nm, collects points with variable precision. We set the RIEGL to scan with a vertical and horizontal resolution of 0.01° to ensure sufficient points and a scantime around 50s for our field of view.

The OUSTER os1-64 records points in 64 channels. Due to the limited channel number, the points recorded on samples are less in comparison to the other scanners. All of the samples are between 1 and 10 cm in size, with the exception of one larger basalt sample.

A laptop running ROS (the Robot Operating System)

We acknowledge funding from the ESA Contract No. 4000130925/20/NL/GLC for the “DAEDALUS – Descent And Exploration in Deep Autonomy of Lava Underground Structures” Open Space Innovation Platform (OSIP) lunar caves-system study and the Elite Network Bavaria (ENB) for providing funds for the academic program “Satellite Technology”.

drivers receives point cloud data from all laser scanners connected via ethernet.

We manually select a point at the center of the sample. Following the calculation of a mean from all values inside a radius, we choose according to the sample size. To limit outliers, we apply a 95% sigma band as in the optical method. The distance difference between the point of interest to laser scanner and the selected center to scanner indicates association to the sample. All differences higher than 1cm are presumably not from the sample and thus we discard them. A calibration of the values to the same four Lambertian targets as in the optical solution enables a comparison of intensity values. Resulting relations allow us to differentiate between the rock samples.

Discussion: All anorthosite samples show an increasing overall reflectance and similar trend, but differ in the slopes between the individual measurements as illustrated in Fig. 1. One explanation is the accuracy of the manual rock selection, which results in deviations from the actual value. By implementing automated detection, we can expect an improvement in both the reflectance values and the shape of the graph.

Water ice has a higher reflectance than anorthosite, but the rock sample with an ice layer has the lowest reflectance values. The cameras do not detect the ice, because it is too thin and thus the graph resembles anorthosite without water ice.

We normalize the mean intensity values from each image with 50% of the maximum reflectance instead of 100% to make them closer to the nominal values and easier to differentiate. Another possibility to improve the results is the use of more halogen lamps for a more uniform illumination.

Our experiments show the ice absorbs the wavelength 1550nm the most (Fig. 2). A resulting slope of 905nm to 1550nm under -15×10^{-5} indicates the presence of H_2O ice. Consequently, we can detect ice too thin for the optical systems, increasing the chance of spotting H_2O on the moon. Obtained results demonstrate slopes that enable a differentiation of the used samples, as seen in Fig. 2 we detected a 905nm to 1550nm slope of around 15×10^{-5} for anorthosite samples in comparison to one around 31×10^{-5} for dunite.

The method we apply to extract the LiDAR intensity values is prone to include points not belonging to the sample. An alternative to improve this approach is to implement an object detection in order to include less background intensity values and more sample values in the equation.

Future field research will refine our methods to distinguish a wider spectrum of rock types and increase the probability of identifying the sample correctly.

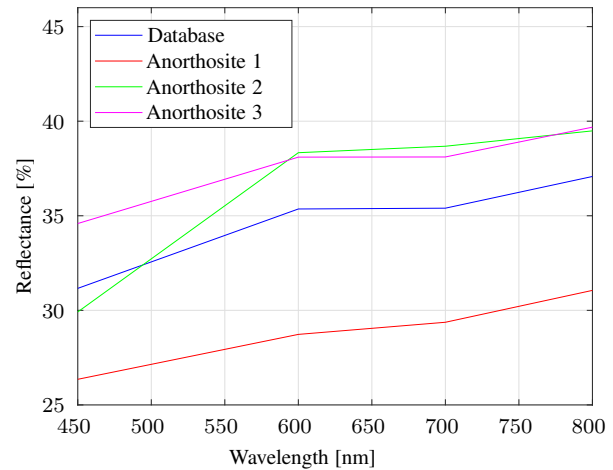


Figure 1: Light reflectance of three terrestrial anorthosite samples and the expected target values at 450nm, 600nm, 700nm and 800nm. Anorthosite 1 has a thin ice layer.

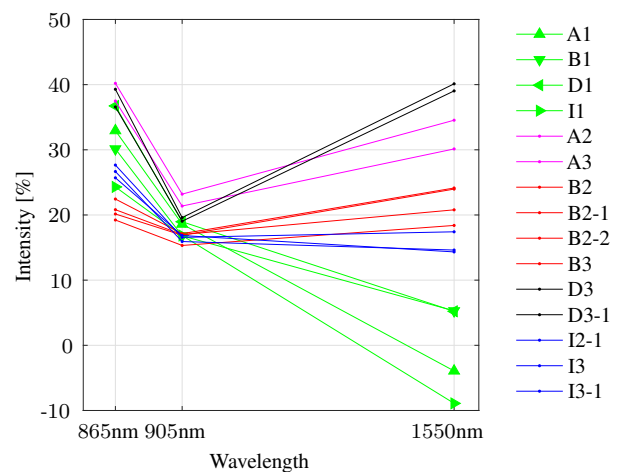


Figure 2: LiDAR intensities for terrestrial rock samples taken with an OUSTER (865nm), LIVOX (905nm), and RIEGL(1550nm) of the types anorthosite (A1, A2, A3), basalt (B1, B2, B2-1, B2-2, B3), dunite (D3, D3-1) and ilmenite (I2-1, I3, I3-1). A1, B1, D1 and I1 are covered with a thin H_2O ice layer. Two of the ice stone values fall into negative space, due to the fact that the measured intensity is lower than the 2% reflectance target we use for calibration.

References: [1] A. P. Rossi et al. *DAEDALUS – Descent And Exploration in Deep Autonomy of Lava Underground Structures*. Uni Wuerzburg Research Notes in Robotics and Telematics. Julius Maximilian University of Würzburg, Mar. 2021, pp. 1–190. [2] NASA PDS Geosciences Node at Washington University in St. Louis. *PDS Geosciences Node Spectral Library*. <https://pds-spectlib.rsl.wustl.edu/>. Accessed: 2023-02-20.